Optics Letters

Sodium guide star laser pulsed at Larmor frequency

Xuezong Yang,[1,2] Lei Zhang,[1,3] Shuzhen Cui,[1] Tingwei Fan,[1,2] Jinyan Dong,[1,2] and Yan Feng[1,*]

[1]Shanghai Key Laboratory of Solid State Laser and Application, and Shanghai Institute of Optics and Fine Mechanics, Chinese Academy of Sciences, Shanghai 201800, China
[2]University of the Chinese Academy of Sciences, Beijing 100049, China
[3]e-mail: zhangl@siom.ac.cn
*Corresponding author: feng@siom.ac.cn

Received 4 July 2017; revised 28 September 2017; accepted 29 September 2017; posted 2 October 2017 (Doc. ID 301512); published 20 October 2017

589 nm lasers pulsed at Larmor frequency, several hundreds of kilohertz, can increase the brightness of a sodium guide star and are required in remote magnetometry with mesospheric sodium. By amplification of a continuous-wave single-frequency 1178 nm laser in a pulse-pumped Raman fiber amplifier and frequency doubling in an external cavity, high-power pulsed 589 nm laser at Larmor frequency is obtained for the first time, to the best of our knowledge. The pulse format is mainly determined by the 1120 nm Raman pump laser, whose pulse repetition rate and duty cycle are adjustable. Active pulse shaping is applied to minimize the relaxation spike at the leading edge of the pulses. A reduction in pulse width and conversion efficiency from 1120 to 1178 nm is observed in the backwardly pumped Raman fiber amplifier due to the pump pulse transition effect. A 589 nm laser pulsed at a 350 kHz repetition rate and 20% duty cycle with average power up to 17 W is demonstrated as an operation example intended for a geomagnetic field of 0.5 G.

OCIS codes: (140.3510) Lasers, fiber; (140.3550) Lasers, Raman; (140.3515) Lasers, frequency doubled.

https://doi.org/10.1364/OL.42.004351

Obtaining high-resolution images of astronomical objects with ground-based large aperture telescopes is hampered by image distortion induced by atmospheric turbulence. An adaptive optics (AO) system can sense and correct atmospheric aberrations in real time [1]. The sodium guide star, generated at ~90 km altitude by 589 nm laser irradiation, is considered as the best choice of AO beacons. It has been widely used in astronomical telescopes [2,3]. The development of 589 nm lasers has been restrained by the lack of solid-state gain medium at this band. Dye lasers, optically pumped semiconductor lasers, and frequency sum mixing of 1064 and 1319 nm Nd:YAG lasers [4–6] have been developed to obtain 589 nm sources; however, these approaches suffer from high maintenance, low power, high complexity, or high cost. More recently, Raman fiber amplifiers (RFAs), with the advantages of high stability, compactness, wavelength agility, and high power, have shown promise for generating 589 nm sodium guide star lasers [7–10].

The brightness of the laser guide star (LGS), which is determined by the power, spectral, temporal, and polarization characteristics of the laser, is a key parameter to maximize the performance of AO systems [11–13]. Sodium guide star lasers, pulsed at magnetic precession frequency—Larmor frequency—can significantly enhance backscatter from a sodium layer and may be used for a laser remote magnetometer [13–15]. Therefore, this kind of laser is of great scientific importance and interest. The Larmor frequency is on the order of several hundreds of kilohertz, proportional to the geomagnetic field. The optimum duty cycle is about 20% according to some simulations [13,15]. The necessary average output is larger than 10 W for usual situations, but a 589 nm laser with a repetition frequency of hundreds of kilohertz is not available and technically challenging, especially with high power. In [13], a solid state approach has been proposed to generate 589 nm laser pulsed at Larmor frequency by frequency sum mixing of a 1064 nm continuous-wave (CW) laser and a 1319 nm Q-switched laser in a LiB_3O_5 (LBO) nonlinear crystal, but it has not yet been demonstrated.

In this Letter, a high-power sodium guide star laser pulsed at Larmor frequency is reported for the first time, to the best of our knowledge. The laser is based on the frequency doubling of a high-repetition-rate pulse-pumped 1178 nm single-frequency Raman fiber amplifier. As an operation example, a pulsed 589 nm laser with 17 W average power is demonstrated at a duty cycle of 20% and a repetition rate of 350 kHz, which is suitable for a geomagnetic field of 0.5 G. Note the pulse repetition rate and duty cycle can be adjusted easily for use in different geographic locations and performance optimization. Pulse width and conversion efficiency reduction in the backwardly pumped sub-μs Raman fiber amplifier due to the pump pulse transition were observed and analyzed for the first time, to the best of our knowledge.

The experimental configuration is shown in Fig. 1. The seed laser is an 1178 nm fiber-coupled distributed feedback (DFB) diode laser, which outputs up to 10 mW with ~1 MHz

Corrected 30 October 2017

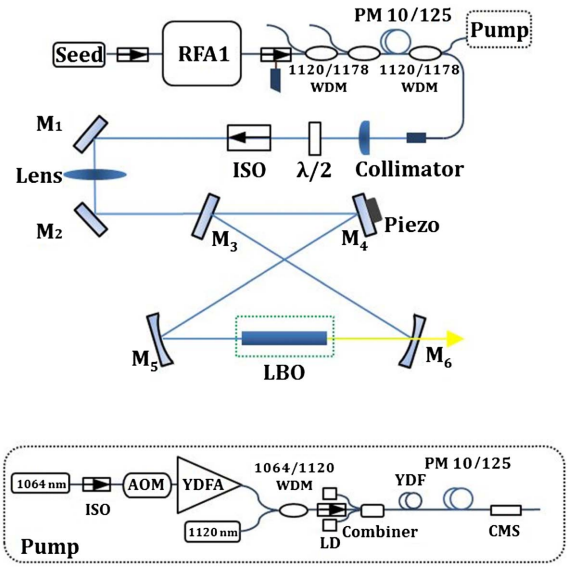

Fig. 1. Diagram of the guide star laser system. The setup of the pump laser for the boost RFA is shown in the dashed box at the bottom of the figure. CMS, cladding mode stripper.

bandwidth. The 1178 nm seed laser is amplified by two stages of RFAs. At each RFA, one PM1120/1178 nm wavelength division multiplexing (WDM) is used for coupling the pump laser into the Raman amplifier, and two WDMs are employed to extract the residual pump lasers. The gain fibers used for the first and second RFAs are 200 m PM980 fiber and 35 m PM10/125 fiber, respectively. Stimulated Brillouin scattering (SBS) is the main technical challenge for power scaling in single-frequency RFAs. PM10/125 fiber is used in the second RFA for its larger mode area, which is helpful in increasing the SBS threshold. The fiber is single mode at 1178 nm. Longitudinally varied strain along the gain fiber is applied to effectively broaden the SBS gain spectrum. Then the SBS light from different portions of the gain fiber is spectrally isolated and not amplified efficiently in other portions of the fiber. Eight and 30 steps of strain are applied to suppress the SBS effect [9,10,16]. The stain steps are the same as those in [10], and a method of applying strains along the fiber is described in [16]. The output from the first stage amplifier is 0.45 W in the experiments.

The second RFA boosts the 1178 nm laser power and defines the pulse format. Besides the SBS suppression, tailoring the output characteristics of the 1120 nm pump laser is the key technical challenge in this Letter. The setup of the 1120 nm pump laser is shown in the dashed box in Fig. 1. The emission wavelength from ytterbium (Yb)-doped fiber (YDF) lasers is limited to a small range around 1060 nm. Amplified spontaneous emission and parasitic lasing at 1060 nm limit the power scaling of 1120 nm lasers with YDF. Here an integrated Yb-Raman fiber amplifier (YRFA) architecture is applied for achieving high-power 1120 nm fiber lasers [10,17,18]. The gain media of the YRFA consist of 4.5 m YDF followed by 8 m Raman gain fiber. The YRFA is seeded with lasers at convenient Yb wavelength and Raman Stokes wavelength, simultaneously.

In a previous report [10], an 1120 nm high-power pulsed laser, with an adjustable repetition rate (500 Hz–10 kHz) and pulse duration (1 ms–30 μs), was achieved by modulating the pump diodes of the YRFA. The technique is not suitable for this Letter because here we aim for high-power pulsed output with a high repetition rate (several hundreds of kilohertz) and narrow duration (hundreds of nanoseconds). Instead, an intensity-modulated seed laser with CW-pumped YRFA is used, which is efficient because the excited-state lifetime of the Yb ions is ∼0.8 ms.

As shown in Fig. 1, the seed laser of the YRFA consists of an intensity-modulated linearly polarized 1064 nm fiber laser with an average power of 5 W and a linearly polarized 1120 nm CW fiber laser with a power of 4.8 W. The 1064 nm seed laser is constructed by external modulation of a CW oscillator with a fiber-pigtailed acousto-optic modulator (AOM) and one stage of YDF amplification. A signal generator is used to control the AOM and the output pulse format of the 1064 nm laser. In the YRFA, both the 1064 and 1120 nm lasers are amplified in the Yb-doped fiber. Then the 1064 nm laser is converted to 1120 nm by stimulated Raman scattering (SRS) in the following fiber.

The target shape of 1120 nm pulses is flat-toped. However, pulse shape evolution is significant in a CW-pumped high-power Yb fiber amplifier due to population dynamics [19]. With square-shaped seed pulses, the amplified pulses have a spike at their leading edge, as shown in Fig. 2(a). By actively adjusting the modulation waveform of AOM to pre-compensate the gain saturation effect, it is possible to achieve rectangular pulses [20]. This pulse-shaping method is implemented in the experiment to obtain approximate rectangular pulses. A typical output pulse and corresponding modulation waveform applied on AOM are illustrated in Fig. 2(b).

The output power curves of the 1120 nm fiber laser are shown in Fig. 3(a). When the pump power increases to 230 W, the average output power reaches 158 W. The CW 1120 nm seed laser and its further amplification in YRFA lead to a significant CW content in the amplifier output. The amount of the CW content can be calculated from the oscilloscope traces of the output. It is found that, at the average output of 158 W, the pulse content is 117 W, and the pulse peak power is about 316 W, with a pulse repetition rate of 350 kHz and a pulse duty cycle of 37%. Figure 3(b) shows the output spectrum, where the residual 1064 nm laser, 1120 nm laser, and further Raman conversion to 1180 nm are observable. The spectral peak at 1120 nm is 20 dB higher than that of 1064 nm. The proportion of 1120 nm laser in the output is about 96.6%, indicating that the Raman conversion from 1064 to 1120 nm is very efficient.

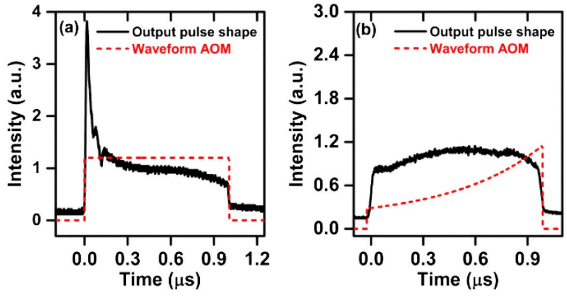

Fig. 2. Pulse shaping of the 1120 nm laser output: (a) square pulse seeding and corresponding output pulse and (b) pre-compensation by shaping the seed pulse with AOM.

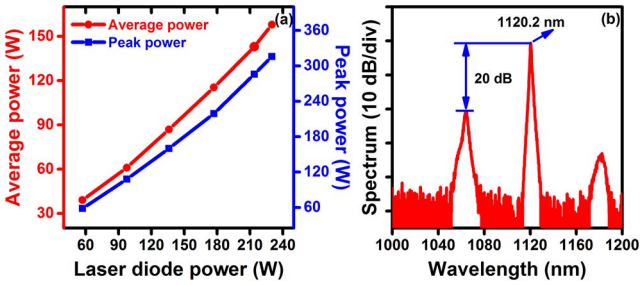

Fig. 3. Output of the high-power 1120 nm laser: (a) the average power and peak power versus the laser diode pump power and (b) the output optical spectrum at a pump power of 230 W.

The 1120 nm high-power pulsed laser is backwardly injected into the second RFA via a WDM. The CW 1178 nm laser is amplified to high-power pulsed output due to the fast response time of SRS. Figure 4(a) shows the 1178 nm output power and backwardly propagating light from the second RFA as a function of pump power. With the increase of pump power, the output power increases to 30 W at a conversion efficiency of 19%. The maximum power of the backward light reaches 1.53 W. Notably, the curve of the backward light power has a steep rise at 1120 nm pump power higher than 143 W, indicating that the SBS reaches threshold. Excessive backward light may result in the damage of optical components, so the 1178 nm output power is limited to 24.7 W during the later experiments. The optical spectrum of 1178 nm laser is measured with an optical spectral analyzer (YOKOGAWA, AQ6370B) with a resolution of 0.02 nm. The spectral signal-to-noise ratio is about 58 dB at the highest power, as shown in Fig. 4(b).

The 1178 nm output pulses are examined in detail. Figure 5(a) shows the pulse trains of 1178 nm laser at different powers, where the pulse repetition rate is 350 kHz, and the pulse duration increases from 305 ns to 730 ns. This pulse width increasing is a result of the 1120 nm pulse changes at different pumping levels. The inset is a single pulse of the 1178 nm laser at a power of 30 W. The trailing edge of the pulse is jittering, which is another evidence of the SBS effect, and its leading edge has a small spike, which is consistent with a 1120 nm pump pulse shape at 158 W.

Figure 5(b) plots the pulse trains of the 1178 nm laser and the corresponding 1120 nm pump laser at a power of 143 W.

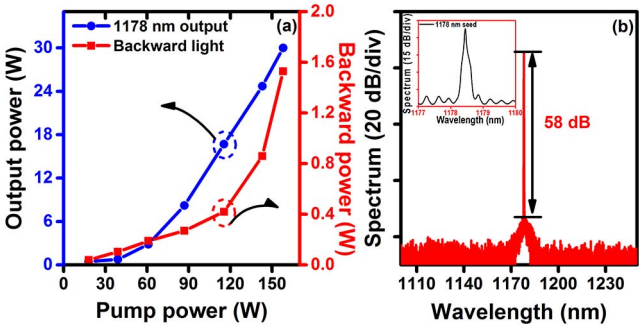

Fig. 4. (a) Power of 1178 nm amplifier output and backward light versus the pump power of the boost RFA; (b) spectra of the 1178 nm RFA output and DFB seed (inset).

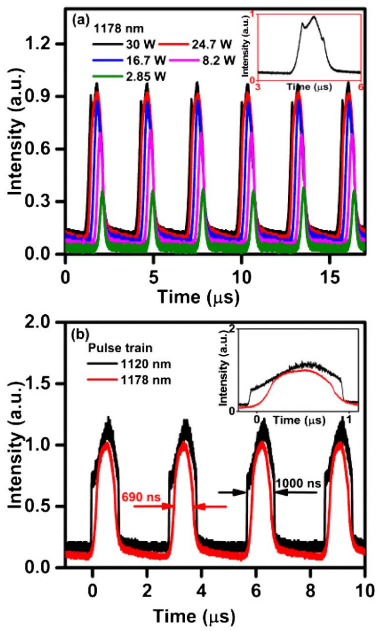

Fig. 5. (a) Pulse trains of 1178 nm laser at different powers and a single pulse at 30 W average power (inset); (b) pulse trains of the 1120 and 1178 nm lasers at 1120 nm laser power of 143 W and single pulses (inset).

It is evident that the 1178 nm pulses have fewer steep edges and narrower widths than the 1120 nm pulses. The pulse full width at half-maximum (FWHM) width of the 1120 and 1178 nm lasers are about 1000 ns and 690 ns, respectively. These changes in pulse waveform are the results of pump pulse transition through the gain fiber in the backwardly pumped Raman fiber amplifier. For a pump pulse of width Δt, the CW signal light experiences full amplification only in the center part of the pump pulse with a duration of $\Delta t - 2nL/c$, where L is the gain fiber length of the second RFA (~35 m), n is the refractive index of the gain fiber, and c is the speed of light in vacuum. The two times transit time, $2nL/c$, is calculated to be 340 ns. It is longer than the observed reduction in FWHM width of 310 ns. This is due to the partial amplification during the transit of pulse edges. The reduction in pulse width accounts for about one-third of the pump pulse duration, which explains the relatively low Raman conversion efficiency (19%) from 1120 to 1178 nm, as compared to our previous CW or long pulse works [10,16].

After a half-wave plate and a free space optical isolator (ISO), the 1178 nm amplifier output is coupled into a homemade external resonant frequency doubling cavity. In the cavity, the frequency doubling crystal is a 3 mm × 3 mm × 30 mm non-critical phase-matched LBO crystal with a phase-matching temperature of 43.5°C. The cavity is locked using the well-established Pound–Drever–Hall method. At a repetition rate of 350 kHz, the output power and second harmonic generation (SHG) efficiency of 589 nm pulsed laser versus 1178 nm input power are shown in Fig. 6(a). With the 1178 nm power increasing up to 22.7 W (measured after ISO), the 589 nm power increases to as high as 17 W, and the conversion efficiency reaches 74.9%. Figure 6(b) shows the pulse trains of the 589 nm laser at different output powers. In the resonant frequency doubling

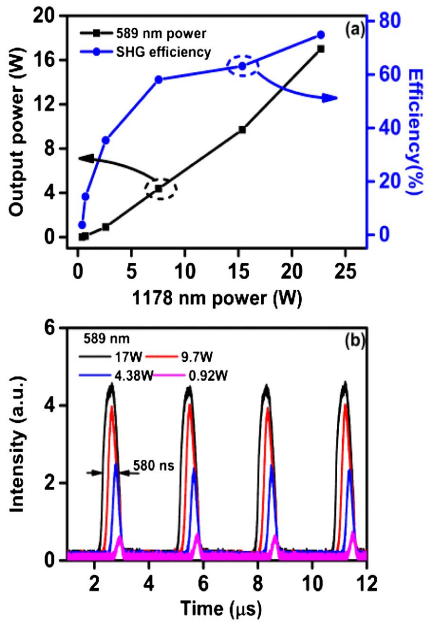

Fig. 6. 589 nm pulsed laser with 350 kHz repetition frequency: (a) the average output power and SHG conversion efficiency as a function of 1178 nm power and (b) pulse trains at different powers.

cavity, the maximum frequency doubling efficiency can be achieved when the incident power matches well with the reflectivity of the incident mirror and effective cavity loss, including the SHG process [21]. Therefore, the low power contents of the 1178 nm input pulse—the pulse edges and the CW base in the pulse interval—have lower frequency doubling efficiency. It is manifested in the 589 nm pulse train that the pulse duration is narrower than that of 1178 nm, and there are fewer CW components (~4%) in the pulse interval. This residual CW component can be removed in later development by modulating the 1120 nm seed laser as well. At the output power of 17 W, the pulse duration is about 580 ns, the pulse duty cycle is 20%, and the pulse peak power reaches 81.4 W. The linewidth should be less than 5 MHz, according to our previous studies, since no linewidth broadening was observed after the Raman fiber amplification [7,10,16].

The repetition rate of 350 kHz in the demonstration is suitable for locations with a geomagnetic field of 0.5 G, Paranal in Chile, for example, where the very large telescopes are installed. The repetition rate should be adjusted when the laser is used in other geographic locations. Furthermore, the pulse duty cycle should be fine-tuned for optimum operation of both sodium LGS and magnetometry. The reported laser system allows easy adjustment of a laser pulse repetition rate and duty cycle by modifying the waveform applied on the AOM. As an example, the laser system has been adjusted to operate with similar output at a repetition rate of 325 kHz (Larmor frequency in Shanghai).

In summary, a 589 nm laser pulsed at Larmor frequency is reported for the first time, to the best of our knowledge. The laser is developed for improving the brightness of sodium LGS and remote magnetometry with mesospheric sodium. As a demonstration, 17 W 589 nm laser is achieved with a 350 kHz pulse repetition rate and 20% duty cycle. The laser system includes amplification of a CW single-frequency 1178 nm laser in a pulse-pumped Raman fiber amplifier and frequency doubling in an external cavity. A reduction in pulse width and conversion efficiency from 1120 to 1178 nm is observed and analyzed in the backwardly pumped Raman fiber amplifier due to the pump pulse transition effect. Further power scaling is possible by improving the Raman fiber amplifier. The results show again the technical flexibility of a Raman fiber-amplifier-based guide star laser.

Funding. National Natural Science Foundation of China (NSFC) (61378026, 61575210).

REFERENCES

1. L. W. Peter, M. David Le, H. B. Antonin, D. C. Randy, C. Y. C. Jason, R. C. Adam, A. V. D. Marcos, K. H. Scott, M. J. Erik, E. L. Robert, L. Hilton, J. S. Paul, M. S. Douglas, G. B. Curtis, M. D. Pamela, E. M. Claire, and M. P. Deanna, Publ. Astron. Soc. Pac. **118**, 297 (2006).
2. W. Happer, G. J. MacDonald, C. E. Max, and F. J. Dyson, J. Opt. Soc. Am. A **11**, 263 (1994).
3. C. E. Max, S. S. Olivier, H. W. Friedman, J. An, K. Avicola, B. V. Beeman, H. D. Bissinger, J. M. Brase, G. V. Erbert, D. T. Gavel, K. Kanz, M. C. Liu, B. Macintosh, K. P. Neeb, J. Patience, and K. E. Waltjen, Science **277**, 1649 (1997).
4. M. Fallahi, L. Fan, Y. Kaneda, C. Hessenius, J. Hader, H. Li, J. V. Moloney, B. Kunert, W. Stolz, S. W. Koch, J. Murray, and R. Bedford, IEEE Photon. Technol. Lett. **20**, 1700 (2008).
5. C. A. Denman, P. D. Hillman, G. T. Moore, J. M. Telle, J. E. Preston, J. D. Drummond, and R. Q. Fugate, Proc. SPIE **5707**, 46 (2005).
6. F. Bos, Appl. Opt. **20**, 1886 (1981).
7. Y. Feng, L. R. Taylor, and D. B. Calia, Opt. Express **17**, 19021 (2009).
8. L. R. Taylor, Y. Feng, and D. B. Calia, Opt. Express **18**, 8540 (2010).
9. L. Zhang, Y. Yuan, Y. Liu, J. Wang, J. Hu, X. Lu, Y. Feng, and S. Zhu, Appl. Opt. **52**, 1636 (2013).
10. L. Zhang, H. Jiang, S. Cui, J. Hu, and Y. Feng, Laser Photon. Rev. **8**, 889 (2014).
11. R. Holzlöhner, S. M. Rochester, D. Bonaccini Calia, D. Budker, J. M. Higbie, and W. Hackenberg, Astron. Astrophys. **510**, A20 (2010).
12. T. Fan, T. Zhou, and Y. Feng, Sci. Rep. **6**, 19859 (2016).
13. T. J. Kane, P. D. Hillman, and C. A. Denman, Proc. SPIE **9148**, 91483G (2014).
14. T. J. Kane, P. D. Hillman, C. A. Denman, M. Hart, R. P. Scott, M. E. Purucker, and S. J. Potashnik, https://arxiv.org/abs/1610.05385.
15. J. M. Higbie, S. M. Rochester, B. Patton, R. Holzlöhner, D. Bonaccini Calia, and D. Budker, Proc. Natl. Acad. Sci. USA **108**, 3522 (2011).
16. L. Zhang, J. Hu, J. Wang, and Y. Feng, Opt. Lett. **37**, 4796 (2012).
17. L. Zhang, H. Jiang, S. Cui, and Y. Feng, Opt. Lett. **39**, 1933 (2014).
18. L. Zhang, C. Liu, H. Jiang, Y. Qi, B. He, J. Zhou, X. Gu, and Y. Feng, Opt. Express **22**, 18483 (2014).
19. W. Yong and P. Hong, J. Lightwave Technol. **21**, 2262 (2003).
20. A. Malinowski, K. T. Vu, K. K. Chen, J. Nilsson, Y. Jeong, S. Alam, D. Lin, and D. J. Richardson, Opt. Express **17**, 20927 (2009).
21. A. Ashkin, G. Boyd, and J. Dziedzic, IEEE J. Quantum Electron. **2**, 109 (1966).